Chapter 4

Functional analysis of the *mpzl3* gene in zebrafish

Racz P, Zakrzewska A, Csukonyi E, Ordas A, Spaink HP, Mink M, Meijer AH,
in preparation

Abstract

MPZL3 is a novel member of the myelin Po protein family. The gene was identified through a mutation in the rough coat mouse strain and is conserved in all vertebrates. Although *in silico* analyses suggest that the gene encodes an adhesion molecule with a possible immunological role, functional analyses have not yet been reported. In this study we investigated the zebrafish homolog of *mpzl3*. We determined the expression pattern of the gene during zebrafish embryo development by whole-mount *in situ* hybridization, and examined the effects of overexpression and morpholino knock-down regulation. Our results show that *mpzl3* has an important role in early developmental processes, and that its overexpression causes major defects in eye development and general retardation of larval development. Knock-down of *mpzl3* using morpholino antisense technology also resulted in several defects, including locomotion disorder, altered head morphology, edema in the eye and the heart, and other cardiovascular abnormalities. Microarray analysis of the effects of *mpzl3* knock-down during early embryogenesis revealed altered expression of genes involved in several developmental processes and suggested that *mpzl3* might be involved in Notch and Wnt signaling.

Introduction

MPZL3 is a novel member of the myelin Po family. The gene was identified at mouse chromosome 9 (Dickie, 1966), at 44, 86 Mb (Cao et al., 2007) through a spontaneous recessive point mutation in an inbred C57BL/6J mouse strain, called rough coat (*rc*) (Cao et al., 2007; Hayashi et al., 2004). The gene encodes a 237 amino acid long polypeptide with an Immunoglobulin V-type domain (IgV). The rough coat mutation causes a single nucleotide transition in the gene and an Arg-Gln substitution within a conserved residue of the functional IgV domain (Cao et al., 2007). RT-PCR analysis revealed that the gene is expressed in a variety of organs like brain, esophagus, heart, intestine, kidney, liver, lung, muscle, skin, and spleen (Cao et al., 2007). The mutated gene in mice causes numerous abnormalities, including growth retardation, severe skin abnormalities, myocardial degeneration, hypercalcaemia, liver inflammation and abnormal hemosiderin granules deposition in the spleen (Hayashi et al., 2004). Although *in silico* based annotation indicates that the protein might play a role in thymus and T cell development (Racz et al., 2009), *in vivo* functional analyses have not yet been achieved. Knock-out analysis in mice will be a useful approach to study the function of the gene. However, given that the rough coat point mutation in *Mpzl3* already has strongly effects, it is possible that the complete lack of *Mpzl3* function may lead to more drastic changes in the affected organ systems and result in a lethal phenotype. Considering the time investment and the possible outcome of the mouse knock-out experiment, we decided first to investigate the *Mpzl3* gene function in the zebrafish embryo model, in which rapid knock-down

studies are possible.

Zebrafish has become a widely used model organism in biology. In the last decade many studies have used zebrafish as a model to better understand human diseases or to investigate functions of genes conserved between fish and human. The zebrafish has several advantages, like easy maintenance, small space requirements, large brood size, and reasonably short life cycle (generation time is about 10 weeks). It is a convenient model organism to do large scale screenings because the females are able to produce 200–300 new progeny every week. As the embryos develop outside the mother and remain translucent for several days, it is possible to visually track every aspect of their development. The embryogenesis is rapid and most organ systems are fully developed by 5 days post-fertilization (dpf). The transparency of the embryos can be exploited to localize specific cell types and developing organs by whole mount *in situ* hybridization (WISH) in fixed embryos, or to monitor developmental processes in real time using fluorochrome tagged cells in living embryos. As the embryos are developing *ex vivo* in the aquarium medium, any soluble molecule can be readily applied and used for example to probe developmental signaling pathways or for testing of pharmacological activity. Furthermore, embryo development can be easily manipulated by micro-injection of messenger RNAs for overexpression studies or by injection of antisense morpholino oligonucleotides for transient gene knock-down. The zebrafish embryo model allows the phenotypic assessment of mutations that in mammals would cause very early embryonic lethality. For example, even drastic cardiovascular defects can be studied, as the embryos can gain sufficient oxygenation via diffusion through the skin during the first days of their development (Grillitsch et al., 2005; Pelster and Burggren, 1996).

Relevant to the study of *mpzl3*, is that the zebrafish immune system has proven to be remarkably similar to that of humans (Traver et al., 2003). Studies of hematopoiesis have revealed that most if not all cell types of the human immune system have zebrafish counterparts (Berman et al., 2003; Traver et al., 2003). Macrophages and neutrophils already develop during the first day of embryogenesis. T cell developmental genes show strong homologies to mammalian genes with similar expression and functional profiles. B cells also exist and express activation-induced cytidine deaminase but do not undergo class-switch recombination (Barreto et al., 2005) and somatic hypermutation is inefficient (Wakae et al., 2006). The thymus in zebrafish is similar to that of mammals with the main exception that the zebrafish thymus remains as two discrete bilateral structures (Meeker and Trede, 2008). T cells exit the thymus and populate various tissues including the kidney, pharynx, intestinal tract, nose, spleen, and skin. In adult fish the hematopoiesis occurs in the kidney which is equivalent to the human bone marrow (Al-Adhami MA, 1977). The zebrafish lymphatic system has also been identified (Kuchler et al., 2006; Yaniv et al., 2006), although they do not have lymphatic nodes, Peyer's patches or splenic germinal centers.

In this study we identified the evolutionary conserved counterpart of mamma-

lian *mplz3* in zebrafish and characterized the expression pattern of this gene during embryo development. We performed overexpression and morpholino knock-down experiments to investigate the function of the *mpzl3* gene. In addition to detailed phenotype analysis of the fish with enhanced or reduced *mpzl3* expression, we used microarrays to investigate the global gene expression changes induced by *mpzl3* knock-down.

Results

Characterisation of the *mpzl3* gene in zebrafish:

Based on the Ensembl database (Ensembl release 56 - Sept 2009 Zv8) the zebrafish *mpzl3* gene (ENSDARG00000079225) is located on chromosome 15 at 47 Mb on the forward strand. According to the NCBI Reference Sequence database (NM_213169.1) the coding sequence of the gene consists of 648 nucleotides and encodes a 215 amino acid long polypeptide. We analyzed the protein sequence using the InterProScan domain prediction program and identified Myelin Po motifs at amino acid positions 13-37, 62-89, and 91-120, and a conserved Immunoglobulin (Ig) V-set domain at amino acid positions 16-99

Phylogenetic analysis:

To determine the evolutionary relation between the myelin Po domain (MyPo) containing proteins of zebrafish we downloaded all proteins with a MyPo domain using the Ensembl 54 - Danio rerio Zv8 database. This dataset was uploaded into the ClustalW multiple sequence alignment program and a phylogenetic tree was made using the Neighbor Joining method, allowing the addition of gaps. The results (Figure 1) show that Mpzl3 (ENSDARP00000103451) is most closely related to Mpz (ENSDARP00000101478; ENSDARP00000056371), Mpzl1 (ENSDARP00000092425) and Mpzl2 (ENSDARP00000032601).

Expression of *mpzl3* in zebrafish:

To analyze *mpzl3* expression during zebrafish development first we carried out quantitative RT-PCR (qRT-PCR) analyses using total RNA. As shown in Figure 2A, the *mpzl3* mRNA levels were highest between the 4-cell and dome stages, probably reflecting maternal expression. Expression of *mpzl3* dropped to a much lower level at 80% epiboly, but remained detectable until at least 5 dpf. For more detailed analyses whole-mount *in situ* experiments were performed to analyze the spatial expression pattern of the *mpzl3* mRNA at different time points during embryo and larval development. We observed that in the early developmental stages (4 cell, 8 cell, and 30% epiboly) the mRNA was ubiquitously expressed (data not shown). At later time points *mpzl3* expression became gradually restricted. At 5 dpf, *mpzl3* expression was specifically detected in different areas of the head, including the anterior neuromasts and the branchial arches. We also recognized *mpzl3* expression in neuromasts of the

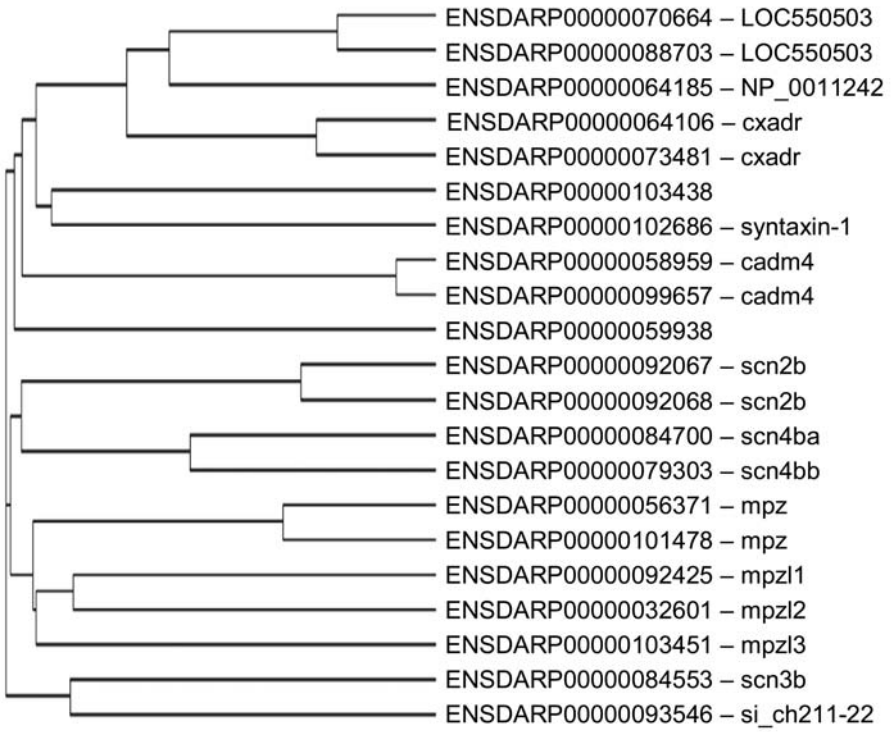

Figure 1. Evolutionary relations of the MyPo domain proteins of zebrafish. The cladogram was made by the ClustalW Neighbour Joining method.

posterior lateral line, in the swim bladder, and the cloaca (Figure 2A).

Overexpression analysis of *mpzl3*:

To investigate the role of *mpzl3* in zebrafish we cloned the *mpzl3* full length coding sequence into the pCS2+ plasmid and used SP6 polymerase to transcribe capped mRNA for micro-injection into embryos at the 1-2 cell stage. Injection of 5 pg mRNA did not induce phenotypic alterations, but injection of 10-75 pg mRNA caused a general retardation of development and edema of the heart cavity was sometimes observed as well as bent and shortened tails. However, the most remarkable and consistent phenotype was aberrant eye development, which was observed in 23% of the embryos injected with 10pg of mRNA and 42% of the embryos injected with the highest amount of mRNA. Embryos injected with the lowest concentration do not show phenotypic difference compare to the uninjected control embryos. Some embryos showed aberrant development of both eyes and others showed asymmetric development of the two eyes, with one developing normally and the other being highly abnormal or completely undeveloped (Figure3).

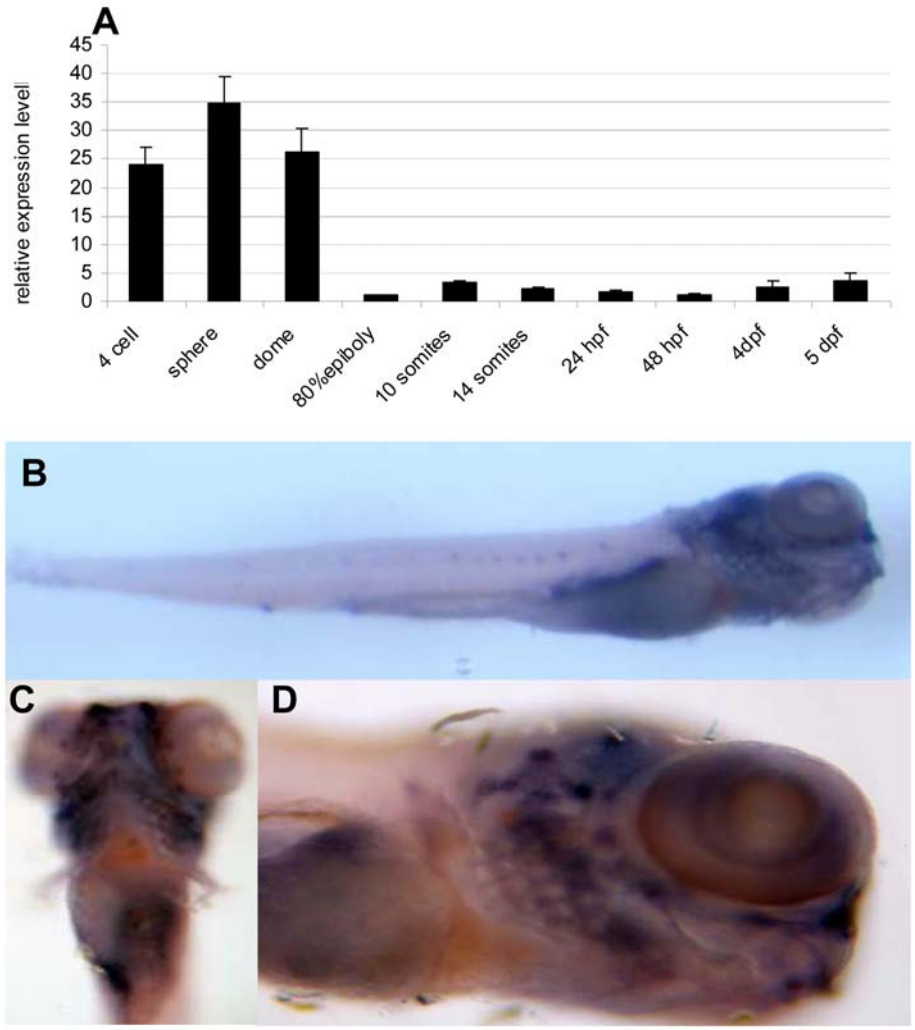

Figure 2. Expression of the *mpzl3* gene in zebrafish embryos. **(A.)** qRT-PCR analysis of *mpzl3* expression. Relative expression levels of *mpzl3* were determined at the indicated developmental stages between the 4-cell stage and 5 dpf. The expression at 80% epiboly is set to 1. Data were normalized to expression of peptidylprolyl isomerase A-like (*ppial*), which showed no changes over the mRNA samples used. **(B-D)**. Expression pattern of *mpzl3* investigated by whole-mount *in situ* hybridization at 5 dpf. *Mpzl3* is highly expressed in the head, including the anterior neuromasts and the branchial arches. Furthermore, *mplz3* expression was detected in the neuromasts of the posterior lateral line, the swim bladder, and the cloaca. Embryos in **(B)** and **(D)** are in lateral view, anterior to the right. A ventral view of the head is shown in **(C)**, anterior to the top.

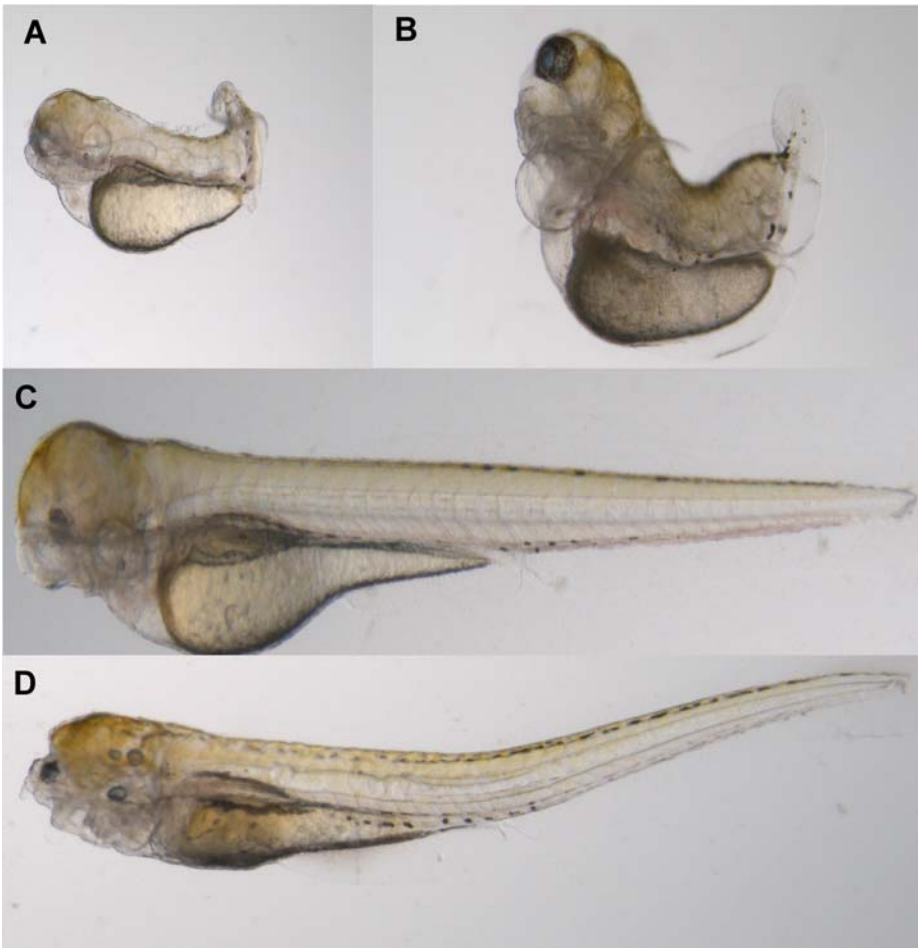

Figure 3. Overexpression analysis of *mpzl3*. Embryos were injected at the 1-2 cell stage with *mpzl3* capped mRNA. **(A)** 3 dpf embryo, injected with 10 pg *mpzl3* mRNA. The embryo shows cardiac edema, a bent tail and only the eye on the right side of the embryo is developed properly. **(B)** 5 dpf embryo, injected with 50pg of *mpzl3* mRNA, the embryo shows cardiac edema, a shortened tail, and only the eye on the left side of the embryo is developed. **(C)** 3 dpf embryo, injected with 10 pg of *mpzl3* mRNA. Here the embryo shows normal tail development, but neither of the eyes was developed. **(D)** 5dpf embryo, injected with 50 pg of *mpzl3* mRNA. Development of the head and both eyes was strongly affected.

Morpholino knock-down analysis of *mpzl3*:

A morpholino knock-down approach was used to block the translation of the *mpzl3* mRNA during zebrafish embryo development (Figure 4). As controls we used non-injected embryos and embryos injected with the standard control morpholino from Genetools. The most conspicuous phenotype that we observed was that injec-

tion of 0.25mM morpholino caused 55 % lethality in the injected population. It was also notable that after hatching a subset of the embryos (4% of 0.1mM morpholino injection, 28% of 0.25mM morpholino injection, and 33% of 0.5mM morpholino injection) lost the ability of movement. We punched these morphants with an acupuncture needle to force them to move in the liquid medium, but the morphants did not react to this treatment. We monitored the phenotype between 3 dpf and 7dpf and no changes were observed during this time (data not shown).

The *mpzl3* morphant fish also developed heart edema at 1 dpf. To further examine this phenotype we used the fli:EGFP transgenic line which expresses green fluorescent protein in the entire vasculatory system. As shown in Figure 4B and 4E-F, the structure of the caudal vasculature of the mpzl3 morphants was affected. A possible explanation for this observation might be that it is a result of the accumulation of erythrocytes in the caudal vasculature region of the morphant fish. We next tested whether the cardiovasculatory defects were associated with any alteration of the heart rate. Therefore, we investigated the heart rate of 10 *mpzl3* morphant fish versus 10 standard control morphants at 7dpf and calculated the average heart beat per minute (bpm). We found that the *mpzl3* morphant embryos had a lower heart rate compared to the controls (90 bpm vs. 155 bpm).

Since Mpzl3 proteins have proposed immune functions, we next tested the hypothesis that *mpzl3* knock-down might affect thymus and T cell development. To this extent we carried out *in situ* hybridization using the recombination activating gene-1 (*rag1*) thymus specific marker (Corripio-Miyar et al., 2007) and found that the *mpzl3* morphant fish do not express the *rag1* marker at 6 dpf, while *rag1* is already detectable in wild type zebrafish larvae at 4 dpf (Figure 4C (Willett et al., 1997).

To test the specificity of the morpholino effect, we designed another translation blocking morpholino (MO2) upstream of the first morpholino (MO1). Repeating all experiments with the second morpholino (MO2), we found that this morpholino (MO2) phenocopied the effects of the first morpholino (Figure 4C-D). In addition, we used the synthetic *mpzl3* mRNA to rescue the morpholino phenotypes by co-injection. We co-injected in the 1-2 cell stage 116 embryos with 10 pg of the *mpzl3* cRNA and 0.125 mM of the *mpzl3*-MO2. After the co-injection the survival rate was elevated from 45 to 84% at day 5. We investigated the ability of fish to move. After 3 days all fish were capable of free swimming and responded to needle punching by swimming away, while more than 20% of the surviving embryos injected with 0.125 mM of *mpzl3*-MO2 showed the motionless phenotype. We also observed that some of the embryos co-injected with *mpzl3* mRNA and morpholino showed undeveloped eye phenotypes (9%) of which more than half also showed heart edema. As eye defects and heart edema were also observed in the overexpression analysis, these phenotypes are probably due to the effect of increased *mpzl3* mRNA level, while the increased survival rate and normal motion of the embryos co-injected with *mpzl3* mRNA and morpholino indicates effective rescue of the morpholino knock-down phenotype.

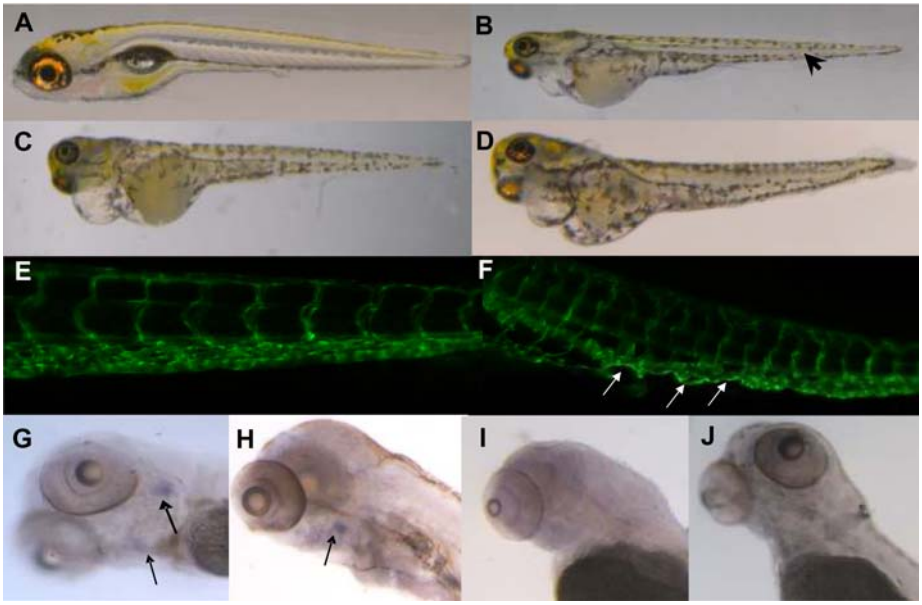

Figure 4. Phenotypes of *mpzl3* morphant fish. **(A-B)** 5 days old wild type **(A)** and embryo injected with 1 nl of 0,25 mM *mpzl3* morpholino (MO1) **(B)**. The morphant fish developed heart edema, and the erythrocytes often accumulated in the caudal region (black arrowhead). **(C,D)** Comparison the effect of the two translation blocking morpholinos MO1 **(C)** and MO2 **(D)**. 1 nl of 0.25 mM concentration was injected for both morpholinos. Embryos are shown at 5 dpf. **(E-F)** Fluorescent microscopy images of the caudal vasculature of wild type **(E)** and MO1 morphant **(F)** fli:EGFP fish. In the morphant fish it is recognizable that the vasculatory system in the caudal part was affected (white arrow) **(G-J)** whole mount *in situ* hybridization of wild type **(G)**, standard control morphant **(H)**, and *mpzl3* MO1 **(I)** and MO2 **(J)** morphants with recombination activating gene-1 (*rag1*) probe at 6 dpf. All images show lateral views, anterior to the left.

Microarray analysis of the *mpzl3* knock-down effect:

To analyze the global gene expression changes that underlie the altered phenotypes caused by *mpzl3* morpholino knock-down, we carried out 4x44k Agilent microarray chip analyses. We investigated the transcriptome level changes in both *mpzl3*-MO1, and *mpzl3*-MO2 morphant fish at 8 hpf, at which time-point phenotypical alterations between morphants and controls could not yet be observed. By choosing this early time-point for our analysis we aimed to gain insight into altered signaling pathways that might be responsible for the later phenotypic defects. As a control we used embryos injected with the standard control morpholino and we analyzed the samples in duplicate with a dye swap. Using the Rosetta Resolver pipeline for normalization and data analysis, we generated an overlapping dataset of the MO1 and MO2 effects versus the standard control. With the significance cut-off at $P \leq 10^{-4}$ level we found that 504 sequences associated with 464 genes were up-regulated

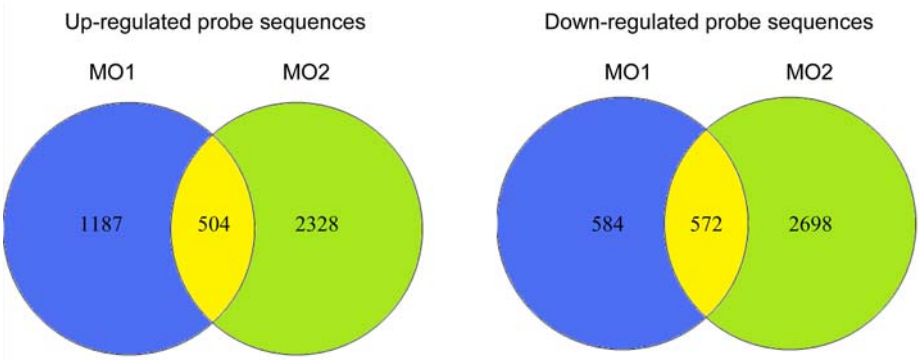

Figure 5. Microarray analysis of the *mpzl3* knock-down effect. **(A)** Venn diagram showing the overlap between the probe sequences up-regulated in embryos injected with *mpzl3* morpholinos MO1 and MO2. The 504 sequences overlapping between MO1 and MO2 corresponded to 464 different genes. **(B)** Venn diagram showing the overlap between the probe sequences down-regulated in embryos injected with *mpzl3* morpholinos MO1 and -MO2. The sequences overlapping between MO1 and MO2 corresponded to 445 different genes. The significance cut off level was $P \leq 10^{-4}$ in both cases.

(Figure 5A) and 572 sequences associated with 445 genes showed down-regulated expression (Figure 5B) with both morpholinos.

To achieve an unbiased functional annotation of the gene set affected by *mpzl3* morpholino knock-down we performed Gene Ontology (GO) analysis using eGOn (explore GeneOntology), a web-based tool for interpreting and statistical analysis of genomic data using GO terms (supplementary Table 1 and 2). The eGOn software classifies user input gene lists by GO criteria for biological process (GO:0008150), cellular components (GO:0005575) and molecular functions (GO:0003674) in a species-independent manner, and produces hierarchical trees of GO terms in these three categories. Among the up-regulated transcripts we observed gene groups associated with negative regulation. For example, we identified negative regulation of cellular processes like, negative regulation of cell cycle (GO:0045786), negative regulation of the signal transduction (GO:0030514, GO:0030178, GO:0040036, GO:0035023), negative regulation of endodermal cell fate specification (GO:0042664) and genes which play a role in the negative regulation of transcription (*her1*, *tp73l*). Genes associated with regulation of apoptosis were also identified by GO analysis. Possibly as the consequence of the enhanced expression of the negative regulation processes, a wide range of developmental processes were also affected, such as liver (GO:0001889), gut (GO:0048547), morphogenesis of the eyes (GO:0048048), skeletal (GO:0001501) and muscle development (GO:0007517). Six genes associated with the morphogenesis of the epithelium (GO:0002009) showed altered expression. Four out of these 6 genes, Bloody fingers (*blf*) Bone morphogenetic protein 2b (*bmp2b*), GLI-Kruppel family member GLI2a (*gli2a*), Nodal-related 2 (*ndr2*) showed upregulated expres-

sion and 2 genes Mix-type homeobox gene 2 (*mxtx2*) and Siaz-interacting nuclear protein (*sinup*) were down-regulated in the *mpzl3* morphants. We also identified several genes involved in development of the brain, where we identified specific *mpzl3* expression by RT-PCR and Western Blot analyses in mouse. Based on the array data the expression level of genes involved in forebrain (GO:0030900), hindbrain (GO:0030902) midbrain (GO:0030901) and diencephalon (GO:0021536) development was increased in *mzpl3* morphants. GO investigation of signal transduction pathways affected by *mpzl3* morpholino knock-down identified eight genes involved in Wnt signaling that showed up-regulated expression. These genes included frizzled homolog 8b (*fzd8b*), dapper homolog 1 (*dact1*), dickkopf 1 (*dkk*), and Sp5 transcription factor-like (*sp5l*) frizzled related protein (*frzb*), frizzled homolog 3 (*fzd3*), casein kinase 2 beta (*ck2b*) sizzled (*szl*), which all showed eleveted expression levels in *mpzl3* morphants. Furthermore, we also identified five signaling molecules that play a role in the Notch pathway. Four out of these five genes, DeltaD (*dld*), Hairy-related 6 (*her6*), Lunatic fringe homolog (*lfng*), and zgc136520,(*zgc136520*) showed up-regulated expression and one gene, disabled homolog 2 (*dab2*), showed down-regulation. In addition, molecules involved in BMP / transforming growth factor beta receptor signaling, MAD homolog 1 and 2 (*smad1* and *smad2*) and sizzled (*szl*), showed up-regulated expression.

Discussion

In this study we performed the first functional analysis of *mpzl3,* a newly identified myelin Po family member in zebrafish and the homolog of the gene mutated in mice with the rough coat phenotype. Overexpression studies showed that elevated levels of *mpzl3* mRNA strongly affected eye development of zebrafish embryos. Knock-down analysis of *mpzl3* using morpholinos resulted in lower survival rates, cardiovasculatory system defects, and affected locomotion of larvae after hatching. Furthermore, expression of the recombination activating gene product (*rag1*) in the thymus was absent in morphant larvae at 6 days postfertilisation. Microarray analysis of the expression pattern changes caused by morpholino knock-down suggested that the Wnt and Notch signaling pathways were affected in addition to the expression levels of several genes involved in developmental processes.

Evolutionary relationships:

Phylogenetic analysis showed that the closest evolutionary related proteins of Mpzl3 in zebrafish are Mpz (myelin protein zero), Mpzl1 (myelin protein zero like 1), and Mpzl2 (myelin protein zero 2) or Eva1 (epithelial V antigen). All three proteins have immunoglobulin V type and myelin Po domains. Comparing this result to data from human and mouse indicates that the members of the family are evolutionary conserved. It is known that EVA1 has the highest sequence homology to MPZL3 in mice (Cao et al., 2007) and plays a role in thymus and early T cell development

(DeMonte et al., 2007; Guttinger et al., 1998). We hypothesized in Chapter 3 that EVA1 and MPZL3 might interact with each other (Racz et al., 2009) and this hypothesis has been supported by a recent large-scale extracellular protein interaction study called AVEXIS (avidity-based extracellular interaction screening) (Bushell et al., 2008). In this study, a systematic screen for receptor-ligand pairs within the zebrafish immunoglobulin superfamily was performed. Two interacting proteins of Mpzl3 were identified, including Eva1 and Cssl:d179; however, the interaction strength between Mpzl3 and Cssl:d179 was one of the weakest measured in this study (Bushell et al., 2008). The other closely related protein, Mpz, is known as the major constituent of the myelin sheath in mammalians, and mutation of *Mpz* causes hereditary motor and sensory neuropathy, called type 1B Charcot-Marie-Tooth disease (CMT). CD8-positive T-lymphocytes were present in mpz mutant mice in the endoneurium (Schmid et al., 2000; Shy et al., 1997). The number of these immune cells increased with time and progression of demyelinating neuropathy, suggesting that the disease might be the consequence of autoimmune inflammation (Maurer et al., 2002).

Mpzl3 expression pattern:

We identified the expression pattern of *mpzl3* in zebrafish embryos and larvae by whole mount *in situ* analyses. Expression of *mpzl3* in embryos at 5 dpf was found to be localized in different areas of the head including the neuromast cells of the anterior lateral line and the branchial arches. We also identified specific expression in the neuromasts of the posterior lateral line, the swim bladder, and the cloaca. The expression in the cloaca is consistent with previous immunohistochemistry results of Bushell et al. (2008), who detected Mpzl3 protein in the pronephric duct of embryos at 53 hpf. Bushell et al. also detected Mpzl3 protein in the epidermis. We did not observe epidermal expression of *mpzl3* mRNA in our *in situ* analysis except for the expression in epidermal cells of the lateral line neuromasts. The lateral line is an organ with hair cells that are involved in reception of mechanical stimuli. It was hypothesized earlier that *mpzl3* plays a role during hair morphogenesis (Cao et al., 2007). The lateral line organ of zebrafish has been used as a model for hair cell loss and regeneration (Ma and Raible, 2009). It is possible that mutation of the protein caused abnormal differentiation not only of the hair-follicles cycling in the skin surface, but also might affect the sensory ability of the secondary sensory structure. The neuromasts are deposited by a migrating primordium that originates from the otic region. At the end of zebrafish embryogenesis, this line comprises 7–8 neuromasts regularly spaced between the ear and the tip of the tail (Gompel et al., 2001). Adhesion molecules like cadherins are required for normal lateral line development. For example, zebrafish embryos in which *cadherin-2 (cdh2)* expression had been knocked down did not develop an appropriate lateral line (Kerstetter et al., 2004) and *cadherin-4 (cdh4)* morphants developed shorter lateral line nerves and a reduced number of neuromasts, suggesting a disrupted migration of the lateral line primordium after the knock-down of adhesion molecules (Wilson et al., 2007). The signaling process

required for normal hair formation and secondary sensory structure involves the Notch and Wnt pathways (Hawkins et al., 2007; Ma and Raible, 2009), where we observed altered expression in our microarray analysis of *mpzl3* morphant fish. In addition, we observed that *mpzl3* morphant larvae were unable to respond to a touch stimulus. The possibility that this phenotype might be due to dysfunction of the lateral line sensory organ requires further investigation.

Overexpression analysis:

The phenotypes caused by overexpression of *mpzl3* were variable but the common phenotypic difference was that the fish developed anophthalmia. The phenotype varied between the formation of two very small and immature eyes and asymmetric eye development, where one eye developed correctly but the other one was missing. The processes involved in eye formation are conserved from the planaria to the vertebrates (Silver and Rebay, 2005) and require the function of several homeobox genes like *ey/pax6*, *toy*, *six3*, and *six6*. Mutation in these genes causes absence or ectopic formation of the eyes (Chow et al., 1999; Czerny et al., 1999; Loosli et al., 1999). In addition to the conservation of such genes involved in eye morphogenesis, several conserved signaling pathways, including the Wnt and Notch pathways that were affected upon *mplzl3* knock-down, also play a role in eye development (Cagan and Ready, 1989; Gage and Zacharias, 2009; Wehrli and Tomlinson, 1998).

Morpholino knock-down analysis:

Gene knock-down of *mpzl3* using two translation blocking morpholinos resulted in severe abnormalities in zebrafish embryos, including lower survival rate, immobility, cardiovascular system defects and expression deficiency of the *rag1* thymus marker. As discussed above, the immobility of *mpzl3* morphants in response to touch stimuli might be related to dysfunction of neuromast cells that showed *mpzl3* expression in wild type embryos. Two other mechanisms can be hypothesized to explain the motionless phenotype. First, as Mpzl3 is protein closely related to Mpz it might play a role in myelin sheet formation or have an effect on the transmission/processing of impulses propagated along the myelinated fiber. Second, as Mpzl3 has been proposed as an immune-related protein, mutation of the gene might lead to autoimmune-derived demyelination of the axons. However, this possibility is perhaps less likely since the adaptive immune system is not yet matured in zebrafish embryos. Interestingly, when mice heterozygously deficient in *mpz* were cross-bred with homozygous null mutants for the recombination activating gene 1 (*rag-1*) or cross-bred with mice deficient in T-cell receptor a-subunit genes (*tcra*) myelin degeneration and impairment of nerve conduction properties was less severe compared to the heterozygously *mpz*-deficient mice without immune cell deficiencies, suggesting that T cells are involved in the demyelinating process of hereditary neuropathy caused by the *mpz* mutation (Schmid et al., 2000). Another study demonstrated that macrophages are actively involved in demyelination in a model for MPZ-caused inher-

ited neuropathies (Carenini et al., 2001). In addition, CD8-positive T-lymphocytes were found in the endoneurium of *mpz* mutants (Shy et al., 1997). Taken together these data provide strong evidence that the immune system plays a role in neuropathies induced by *mpz* mutation. The possible involvement of *mpzl3* in neurodegenerative disorders needs to be further studied. In zebrafish a screen was performed for mutations that affect myelin gene expression in Schwann cells and oligodendrocytes. This screen identified the motionless mutation *(mot)*, associated with the absence of the myelin basic protein (Mbp) expression and vascular defects. The mutated fish died around 4 dpf probably due to vasculatory system malfunction (Kazakova et al., 2006). Another study in zebrafish shows that mutations affecting neurogenesis are often associated with cardiovascular defects, like in the *natter* (*nat*), *viper* (*vip*), *otter* (*ott*), *fullbrain (ful),* and *snakehead (snk)* mutants (Jiang et al., 1996). In our study of *mzpl3* morphants, in addition to the motility defect, heart edema was also observed, with vasculatory system structure alteration. To investigate the possible relation of *mpzl3* with the immune system we determined *rag1* expression in the morphant embryos. In morphants at 6 dpf obtained with two different *mpzl3* morpholinos, no *rag1* expression could be detected. It is very unlikely that the *rag1* deficiency was the consequence of a developmental delay, as the control fish showed *rag1* expression in the thymus at day 4, consistent with the reported *rag1* expression pattern (Willett et al., 1997). Therefore, the lack of *rag1* expression in *mpzl3* morphants might be the first direct experimental support that the vertebrate Mpzl3 proteins are involved in immune system processes. Based on these results, it would be of great interest to investigate *rag1* expression and T cell functions in the *rough coat* mutant mice.

Microarray analysis of the *mzpl3* knock-down effect:

We performed a preliminary microarray analysis to identify the gene expression pattern changes that may underlie the altered phenotypes caused by the *mpzl3* morpholino knock-down. To avoid secondary effects of the altered embryo morphology, the microarray analysis was performed at 8 hpf, prior to detectable phenotypical differences between morphants and controls. Gene ontology term based classification of the gene set showing altered expression with both *mzpl3* morpholino treatments showed that this set included genes involved in developmental processes that were affected in embryos with altered *mpzl3* expression and/or in the rough coat mice. For example, the rough coat mice show severe skin abnormalities and the morphant embryos showed up-regulated expression of genes associated with the morphogenesis of the epithelium, including *blf*, *bmp2b*, *gli2a,* and *ndr2*. In addition, *ndr2* mutation caused a cyclopia phenotype in zebrafish (Rebagliati et al., 1998), indicating an important role of this gene in eye developmental processes, which we found to be affected by *mzpl3* overexpression. In future work, it would be of interest to extend the overexpression study with microarray analysis for comparison with the results of morpholino knock-down. Another up-regulated gene linked with developmental processes altered in rough coat mice is fibulin 4 (*fbln4*). Based on Gene Ontology

FBLN4 associated with wound healing and plays a role in elastogenesis as it interacts with the propeptide of Lysyl oxidase (LOX), which efficiently promotes assembly of LOX onto tropoelastin (Horiguchi et al., 2009). In the *mpzl3* mutated rough coat mice Lysyl oxidase like molecule (LOXL) was expressed at reduced level (Hayashi et al., 2004). Finally, AP-2 alpha (tfap2a) involved in melanocyte differentiation was also up-regulated in the microarray analysis. In rough coat mice melanocyte color changes were observed in the hair follicles (Hayashi et al., 2004).

As we collected our RNA samples for microarray analysis at 8 hpf and the thymus developmental processes do not start before 60 hpf (Willett et al., 1999), not surprisingly we found only two differentially expressed genes associated with immune system gene ontology terms: sprouty4 (*spry4*) and interleukin enhancer binding factor 2 (*ilf2*), which were upregulated in the morphants. Sprouty 4 is an antagonist of Fgf and Ras/Map kinase signaling and has an important role in embryonic development (Furthauer et al., 2001). Interleukin enhancer binding factor 2, also known as nuclear factor of activated T-cells (NFAT), is one of the several transcription factors required for T-cell expression of the interleukin 2 (IL-2) gene. IL-2 is a key cytokine for T cell activation and its absence caused lethal autoimmunity in mice (Ma et al., 2006), while reduced levels of IL-2 protein caused autoimmune disorders (Crispin and Tsokos, 2008; Setoguchi et al., 2005). In zebrafish ilf2 expression was increased in regenerating fin tissue following amputation(Yoshinari et al., 2009), but its function in zebrafish is currently unknown.

Because the *mpzl3* morphant fish developed heart edema and the rough coat mice developed cardiac muscle fiber disorientation and multifocal myocardial degeneration (Hayashi et al., 2004), we hypothesized that the expression of genes involved in heart developmental processes might be changed in our microarray analysis. Our gene set contained four genes related to heart development: DAZ interacting protein 1 (*Dzip1*), bone morphogenetic protein 2b (*bmp2b*) floating head (*flh*) and nodal-related 2 (*ndr2*). Interestingly, bone morphogenetic protein plays a role in heart development but together with Hedgehog (Hh) also acts as a negative regulator of thymocyte development (Varas et al., 2003).

Finally, the mpzl3 morphant embryos also showed altered expression of genes involved in two conserved signaling pathways. Eight genes involved in Wnt signaling were down-regulated and five genes of the Notch pathway showed up-regulated (4 genes) or down-regulated (1 gene) expression. Both signaling pathways play a role in early embryonal development. Wnt genes encode a large family of secreted glycoproteins that are involved in a wide spectrum of cell activities (Miller, 2002). Wnt receptor binding is tightly modulated through association with diverse secreted proteins, like Dickkopf (Niehrs, 1999), Frzb-1 (Leyns et al., 1997; Wang et al., 1997) or Cerberus (Leyns et al., 1997), and through association with glycosaminoglycans. In addition to the essential role in embryonic patterning, the Wnt canonical pathway also plays a role in cell fate determination, and non-canonical Wnt signaling is required for regulation of planar cell polarity, cell adhesion, and motility (Katoh, 2008).

Wnt signaling also plays a role in T-cell development in the thymus. Using wnt1 and wnt4 double knock-out mice it was shown that after 15-16 days of gestation the number of the thymocytes was reduced by 50-70% (Mulroy et al., 2002). The Notch signaling pathway, which was also affected in mzpl3 morphants, plays multiple roles in the development of the central nervous system including the regulation of neural stem cell (NSC) proliferation, survival, self-renewal and differentiation (Gaiano and Fishell, 2002; Lathia et al., 2008). Notch signaling also regulates keratinocyte proliferation, and commitment and differentiation decisions in the skin (Blanpain et al., 2006; Lee et al., 2007), and contributes to maintenance of the follicular structure of the hair (Demehri and Kopan, 2009). Furthermore, Notch signaling also activates T lineage differentiation from hemopoietic progenitors (Tydell et al., 2007) and has an important role in autoimmune disease through a non-canonical signaling pathway (Talora et al., 2008). The possible link of *mpzl3* with Wnt and Notch signaling suggested by our microarray data is of great interest for further investigation.

Conclusion

In this study we investigated the function of *mpzl3* using overexpression and morpholino knock-down analysis in zebrafish embryos. Taken together, the experimental data suggested that *mpzl3* plays a role in developmental processes during early embryogenesis, which has not been previously reported in mammalians. The *mzpl3* mutation in rough coat mice is a hypomorphic mutation. A null mutant of *mzpl3* has not been described in mammalians, and based on the results of *mpzl3* knock-down in zebrafish might be embryonic lethal. Although the zebrafish study did not provide strong support for our previous hypothesis that *mzpl3* may have an immune function (Racz et al, 2009), a link with the immune system was suggested by the lack of *rag1* expression in *mplz3* morphants. Furthermore, the motility defects in *mplz3* morphants might be related to defects in the formation or maintenance of myelin sheaths, which also requires the function of the closely related *mpz* gene. Our microarray analysis of *mpzl3* morphants suggested alterations in Wnt and Notch signaling processes, which might underlie the observed developmental phenotypes. As Wnt and Notch signaling are also important for skin and nervous system development and immunological processes, the altered regulation of these pathways provides a useful lead for further investigations in the zebrafish and rough coat mouse models

Materials and Methods

Characterization of the zebrafish Mpzl3 protein:

The NCBI (http://www.ncbi.nlm.nih.gov/) and Ensembl (http://www.ensembl.org/index.html) databases were used for gene structure and sequence analyses. For deriving the protein sequence the translate tool accessible on the ExPASy proteomics server was used. Mpzl3 domain structure was identified with EBI-InterProScan

(http://www.ebi.ac.uk/Tools/InterProScan/) software.

Phylogenetic analysis:

By means of MART export using the Ensembl release 54 - May 2009 database (http://www.ensembl.org/biomart/index.html) all the PR00213 - PRINTS fingerprints database records (Myelin_P0 domain) in zebrafish (Ensembl54 Danio rerio Zv8-dataset) were listed. The list was manually complemented with the Mpz, Mpzl1, and Mpzl3 protein sequences. The alignment and the phylogenetic tree were made using the ClustalW multiple sequence alignment program (http://www.ebi.ac.uk/Tools/kalign/index.html) and the neighbor joining method.

Zebrafish strains and husbandry:

Zebrafish were handled in compliance with the local animal welfare regulations and maintained according to standard protocols (zfin.org). Experiments were performed with ABxTL zebrafish and the fli:EGFP transgenic line was used to investigate the cardiovasculatory system of the morphant fish. Embryos were grown at 28.5–30°C in egg water (60 µg/ml Instant Ocean sea salts). Embryos used for whole mount *in situ* staining were kept in egg water containing 0.003% 1-phenyl-2-thiourea (Sigma-Aldrich) to prevent melanization.

RNA isolation:

Embryos for RNA isolation were snap-frozen in liquid nitrogen and subsequently stored at -80°C. Embryos were homogenized in 1 ml of TRIzol reagent (Invitrogen), and subsequently total RNA was extracted according to the manufacturer's instructions. The RNA samples were incubated for 20 min at 37°C with 10 U of DNaseI (Roche Applied Science) to remove residual genomic DNA before purification using the RNeasy MinElute Cleanup kit (Qiagen) according to the RNA clean-up protocol. Total RNA concentrations were determined spectrophotometrically using a Nanodrop ND-1000 (Isogen Life science). Optical density A260/A280 ratios of all samples ranged from 1.8– 1.9, indicating high purity.

Whole-mount *in situ* hybridization:

Embryos were fixed overnight in 4% paraformaldehyde in PBS at 4°C and whole-mount *in situ* hybridization using alkaline phosphatase detection with BM purple substrate (Roche) was performed according to Thisse et al. (45). Total RNA was used to generate templates for riboprobes synthesis by PCR using *mpzl3* gene-specific primers sets including the binding site for T7 RNA polymerase in the reverse primer: FW primer: 5'TGGTCTCCAGCAGAGGTCAGT3', REV primer: 5'TAATACGACT CACTATAGGGTGGTGTGTTCATGCAGTTTG3'. As a marker for the thymus we used recombination activating gene-1 (*rag1*): The sequences of the primers for *rag1* probe synthesis were: FW primer: 5'ATGGCATCACCATCTTCCAGGAAC3', REV primer: 5'TAATACGACTCACTATAGGGTATTGACAGAGTTGGTCAGGGCAG

3'. Digoxigenin-labeled riboprobes were synthesized using the labeling mixes from Roche and Ambion MEGAscript reagents for in vitro transcription.

cDNA synthesis and quantitative real-time PCR:

cDNA synthesis reactions were performed in a 40µl mixture of 1000 µg of RNA, 8 µl of 5x iScript reaction mix (Bio-Rad Laboratories), and 2 µl of iScript reverse transcriptase (Bio-Rad Laboratories). The reaction mixtures were incubated at 25°C for 5 min, 42°C for 30 min, and 85°C for 5 min. Real-time PCR was performed using the Chromo4 Real-time PCR detection system (Bio-Rad Laboratories) according to the manufacturer's instructions. Each reaction was performed in a 25-µl volume comprised of 1 µl of cDNA, 12.5 µl of 2x iQ SYBR Green Supermix (Bio-Rad Laboratories), and 10 pmol of each primer. Cycling parameters were 95°C for 3 min to activate the polymerase, followed by 40 cycles of 95°C for 15 s and 60°C for 45 s. Fluorescence measurements were taken at the end of each cycle. Melting curve analysis was performed to verify that no primer dimers were amplified. All reactions were performed as technical duplicates. For normalization, peptidylprolyl isomerase A-like (*ppial*) was taken as reference (Stockhammer et al., 2009). Results were analyzed using the $\Delta\Delta Ct$ method. Sequence of *mpzl3* forward primer: 5'GCTGCTGCTACTTCAAGGACTC3' and *mpzl3* reverse primer: 5'TGTGACTCTGTGATGGTGTGTTC3'.

Overexpression experiments:

Mpzl3 cDNA was cloned by RT-PCR on RNA from zebrafish embryos using the Superscript III one tube PCR system with Platinum taq (Invitrogen). Primers were designed to contain EcoRI and BamH1 restriction sites (FW:5'-CGGATCCTCACC ATGTCGGTGTGGTCTCCAGCAGAGG-3'; REV: 5'-GGTGAATTCCTAACACT-GTGACTCTGTGATGG-3') for cloning into pCS2+ vector (http://sitemaker.umich.edu/dlturner.vectors/home). The pCS2+-mpzl3 construct was checked by sequencing performed by ServiceXS (Leiden, The Netherlands). To generate *in vitro* capped RNA for micro-injection the pCS2+-mpzl3 plasmid was digested with BamHI and EcoRI restriction endonuclease and used as a template for RNA synthesis using SP6 polymerase according to the mMessage mMachine kit protocol (Ambion). Embryos at the 1 to 2 cell stage were injected with 1 nl containing 5 -75 pg mRNA.

Morpholino knock-down experiments:

Morpholino oligonucleotides (Gene Tools) were diluted to desired concentrations in 1 Danieu's buffer (58 mM NaCl, 0.7 mM KCl, 0.4 mM $MgSO_4$, 0.6 mM $Ca(NO_3)_2$, 5.0 mM HEPES (pH 7.6)) containing 1% phenol red (Sigma-Aldrich). To block translation of the *mpzl3* mRNA, we injected between 0.1 mM (0.85 ng) and 1 mM (8.4 ng) per embryo at the 1 to 2 cell stage. Morpholino sequences were: 5'-CTGCTGGAGACCACACCGACATGC-3' (MO1) and 5'-AACCCGGAAGTGAA-GAAAACACACC-3' (MO2). To control for aspecific morpholino effects, we used the standard control morpholino from Gene Tools.

Microscopy:

Images were taken using Leica M165C stereo and MZ16FA stereo fluorescence microscopes equipped with a DFC420C camera. Images were processed using Leica application suite (LAS) software.

Microarray analysis:

For microarray analysis embryos were injected at the 1-2 cell stage with 0.25 mM of MO1, 0.125 mM of MO2 or 0.25 mM of the standard control morpholino and RNA was isolated at 8 hpf. RNA (cRNA) was synthesized in one amplification round from 500ng of total RNA using the Agilent Two color Quick Amp kit. The dual-color hybridization of the microarray chips was performed according to Agilent protocol G4140-90050 version 5.7 (www.Agilent.com) for two-color microarray-based gene expression analysis. Labeled RNA from embryos injected with MO1 or MO2 was hybridized against RNA from embryos injected with the standard control morpholino. The hybridizations were performed in duplicate with a dye swap. Microarray data were processed from raw data image files with Feature Extraction Software 9.5.3 (Agilent Technologies). Processed data were subsequently imported into Rosetta Resolver 7.0 (Rosetta Biosoftware) and subjected to default ratio error modeling. The data were analyzed at the level of the individual probe sequences. Gene ontology (GO) analysis was performed using the GeneTools eGOn v2.0 web-based gene ontology analysis software (www.genetools.microarray.ntnu.no).

Acknowledgments

This work was partially supported by the European Commission Sixth Framework Program ZF-TOOLS (LSHG-CT-2006-037220). We thank Oliver Stockhammer, Peter Schoonheim, and Chao Cui for helpful discussions and Ulrike Nehrdich, Karen Bosma, and Davy de Witt for zebrafish care.